AIMS Mathematics, 9(1): 2389–2410.
DOI: 10.3934/math.2024118
Received: 30 October 2023
Revised: 22 November 2023
Accepted: 26 November 2023
Published: 25 December 2023

http://www.aimspress.com/journal/Math

Research article

Design and experimentation of sampled-data controller in T-S fuzzy systems with input saturation through the use of linear switching methods

YeongJae Kim, YongGwon Lee, SeungHoon Lee*, Palanisamy Selvaraj, Ramalingam Sakthivel and OhMin Kwon*

School of Electrical Engineering, Chungbuk National University, Cheongju 28644, Republic of Korea

* **Correspondence:** Email: acafela@cbnu.ac.kr, madwind@cbnu.ac.kr; Tel: +820432612422.

Abstract: In this study, the stability and stabilization analyses are discussed for Takagi-Sugeno (T-S) fuzzy systems with input saturation. A fuzzy-based sampled-data control is designed to stabilize the T-S fuzzy systems. Based on the Lyapunov method and some integral inequality techniques, a set of sufficient conditions is obtained as linear matrix inequality (LMI) constraints to guarantee the asymptotic stability of the considered system. In this process, the linear switching method is utilized to design a controller that is dependent on the membership function, and an integral inequality is utilized. Additionally, determination of the controller parameters is achieved by resolving a series of LMI constraints. The effectiveness of these criteria is demonstrated through a real system that is modeled by the T-S system.

Keywords: input saturation; linear matrix inequality; Lyapunov stability; sampled-data control; T-S fuzzy system
Mathematics Subject Classification: 34A07, 34D20, 93D20

1. Introduction

The Takagi-Sugeno (T-S) fuzzy model has emerged as a useful framework for controlling and analyzing complex nonlinear systems [1]. The T-S fuzzy approach approximates the original nonlinear system by dividing a nonlinear dynamic system into a set of linear subsystems through the use of IF-THEN rules, and by combining a series of models via a membership function. Therefore, many researchers have utilized the T-S fuzzy approach by establishing the Lyapunov functions to provide the stability criteria of nonlinear systems [2–4]. For instance, Kwon et al. [3] used the augmented Lyapunov-Krasovskii functionals (LKFs) to derive the delay-dependent stability and stabilization criteria for T-S fuzzy systems as linear matrix inequalities (LMIs). Previous work [4] investigated the problem of memory-based sampled-data control for T-S fuzzy chaotic systems.

On the other hand, as modern high-speed computers and network technologies continue to advance, sampled-data control systems have increasingly become the focus of research and application [5, 6]. Typically, in the implementation of sampled-data control systems, control signals are updated only at discrete sampling instants, offering reduced data consumption and better bandwidth performance. Hence, the study of sampled-data control for T-S fuzzy systems has considerable realistic significance. At present, there are various methodologies to deal with sampled-data control systems, such as discrete-time technique [7], impulsive control approach [8] and input delay method [9]. In recent years, lots of meaningful stabilization results on T-S fuzzy systems with fuzzy sampled-data control achieved via an input delay method have been presented [10–21]. In the field of sampled-data system stability, several methods have been used. These methods are the time-dependent Lyapunov functional technique [10, 11], discontinuous Lyapunov functional approach [12, 13], looped-functional-based approach [14,15], free-matrix-based time-dependent discontinuous Lyapunov functional approach [16, 17], two-sided looped-functional approach [18] and sampling-instant-to-present-time fragmentation method [19]. As shown in these papers, various Lyapunov approaches have been made to derive a less conservative result and determine a maximum upper bound of the sampling period. These methods have been applied to problems in many systems with sampled-data controls, as seen in [20, 21]. In addition, the Lyapunov method in the T-S fuzzy system has also been developed, particularly with various studies focusing on membership function-based LKFs. In the past years, many stability conditions have been obtained on the fuzzy control issue of nonlinear systems via various LKFs [22–30]. For instance, Tanaka et al. [22] obtained the stability and stabilization conditions of fuzzy control systems based on multiple LKFs. Wang and Lam [5] proposed a switching idea to ensure that the differential of the membership function was negative, resulting in less conservative results. Zhang et al. [25] designed membership function-dependent LKFs for T-S fuzzy systems to obtain the stability and stabilization conditions, effectively reducing conservatism while significantly increasing the number of decision variables. Yang et al. [27] studied the issue of the sampled-data stabilization of uncertain fuzzy systems by using a membership function dependent approach. Furthermore, saturation nonlinearity can be caused by the constraints of magnitude and the rate of the actuator inputs [31]. Ignoring input saturation in a control design can severely degrade the closed-loop control performance and lead to instability. Recently, only a few studies have dealt with the problem of T-S fuzzy systems with input saturation [31–33].

Motivated by the above discussions, this paper investigates the problem of stability and stabilization for T-S fuzzy systems with sampled-data control and input saturation. The criteria are derived under the framework of LMIs to guarantee the asymptotic stability and stabilization of the system. The following points are the contributions of this work:

- Appropriate looped-functionals for the sampled-data system are constructed, and some advanced integral inequalities derived from Jensen and Wirtinger-based integral inequalities are utilized.
- The proposed control design takes into account the actuator saturation effect and minimizes implementation costs. Due to this, the proposed control design is suitable for practical implementation.
- To facilitate the analysis of nonlinear sampled-data systems, a T-S fuzzy modeling approach is applied, and a linear switching method is used to extend the viable inter-sampling period.

Finally, experimental results with a rotary inverted pendulum (RIP) model are given to demonstrate the effectiveness of the proposed sampled-data control design via the T-S fuzzy approach.

Notation: $\mathbb{R}^n$ and $\mathbb{R}^{m\times n}$ respectively represent the n-dimensional Euclidean space and $m \times n$ real matrices. $\mathbb{S}_+^n$ and $\mathbb{S}^n$ are the set of symmetric positive definite and symmetric matrices, respectively. $X > 0$ and $X \geq 0$ respectively signify that the matrix X is a real symmetric positive definite matrix and positive semi-definite matrix. I_n denotes the $n \times n$ identity matrix. 0_n and $0_{m\times n}$ denote the $n \times n$ and $m \times n$ zero matrices, respectively. $diag\{\cdots\}$ denotes the block diagonal matrix. $*$ represents the elements below the main diagonal of a symmetric matrix. $X_{[f(t)]} \in \mathbb{R}^{m\times n}$ indicates that $X_{[f(t)]}$ is the matrix with respect to $f(t)$, i.e., $X_{[f_0]} = X_{[f(t)=f_0]}$. $Sym\{X\}$ denotes $X + X^T$.

2. Problem statements

Consider the following class of continuous-time T-S fuzzy systems.

Plant rule a : If $\varsigma_1(t)$ is M_{i1} and $\cdots$ and $\varsigma_p(t)$ is M_{ip}, then

$$\dot{x}(t) = A_a x(t) + B_a u(t), \tag{2.1}$$

where $x(t) \in \mathbb{R}^n$ is the state vector, and $u(t) \in \mathbb{R}^m$ is the input vector. $A \in \mathbb{R}^{n\times n}$, $B \in \mathbb{R}^{n\times m}$ are the system's constant matrices. $\varsigma(t) = \left[\varsigma_1(t), \cdots, \varsigma_p(t)\right]$ is a premise variable which is assumed to be independent of the input $u(t)$ explicitly. r is the number of IF-THEN rules. And, $M_{ik}(a = 1, \cdots, r, k = 1, \cdots, p)$ denotes the fuzzy sets.

The defuzzified fuzzy systems, expressed in (2.1), and their dynamics are outlined as

$$\dot{x}(t) = \sum_{a=1}^{r} \psi_a(\varsigma(t)) \left(A_a x(t) + B_a u(t)\right), \tag{2.2}$$

where $\psi_a(\varsigma(t))$ is the normalized membership function that satisfies the following description:

$$\psi_a(\varsigma(t)) = \frac{\vartheta_a(\varsigma(t))}{\Sigma_{b=1}^{r} \vartheta_b(\varsigma(t))}, \quad \vartheta_a(\varsigma(t)) = \prod_{k=1}^{p} M_{ik}(\varsigma(t)), \tag{2.3}$$

in which $M_{ik}(\varsigma(t))$ is the grade of membership of $\varsigma(t)$ in M_{ak}. And, $\vartheta_a(\varsigma(t))$ is satisfied with

$$\vartheta_a(\varsigma(t)) \geq 0, \quad \sum_{a=1}^{r} \vartheta_a(\varsigma(t)) > 0, \quad \forall t \geq 0. \tag{2.4}$$

In fuzzy system modeling, it is consistently assumed that

$$0 \leq \psi_a(\varsigma(t)) \leq 1, \quad \sum_{a=1}^{r} \psi_a(\varsigma(t)) = 1, \quad \sum_{a=1}^{r} \dot{\psi}_a(\varsigma(t)) = 0. \tag{2.5}$$

Additionally, to guarantee that $\dot{P}_h \leq 0$, where P_a represents constant matrices, $\dot{P}_h$ can be expressed as follows.

$$\dot{P}_h = \sum_{a=1}^{r} \dot{\psi}_a(\varsigma(t)) P_a = \sum_{k=1}^{r-1} \dot{\psi}_k(\varsigma(t))(P_k - P_r). \tag{2.6}$$

A switching idea [5] is used as follows:

$$\begin{cases} \dot{\psi}_k(\varsigma(t)) \leq 0 : P_k - P_r \geq 0, \\ \dot{\psi}_k(\varsigma(t)) > 0 : P_k - P_r < 0. \end{cases} \tag{2.7}$$

In (2.7), there exist 2^{r-1} scenarios. Let S_p denote the set comprising all feasible permutations of $\psi_k(\varsigma(t))$, where $p \in \mathfrak{S}$, $\mathfrak{S} = \{1, 2, \cdots, 2^{r-1}\}$ and C_p is the set that contains the constraints of X_a. So, the inequalities of (2.7) can be presented as follows:

$$\text{if } S_p, \text{then } C_p. \tag{2.8}$$

The control signal is generated according to a consecutive sampling time sequence $0 \leq t_0 < \cdots < t_k < \cdots < \infty$ by using a zero-order hold function. It is subject to the constraint that the sampling period satisfies that $t_{k+1} - t_k = h_k \leq h_M$.

The subsequent sampled-data control method is adopted for the system (2.2).

Controller rule b ($b = 1, 2, \cdots, r$): If $\varsigma_1(t)$ is M_{i1} and $\cdots$ and $\varsigma_p(t)$ is M_{bp}, then

$$u(t) = K_b x(t_k), \qquad t \in [t_k, t_{k+1}), \tag{2.9}$$

where $K_b \in \mathbb{R}^{m\times n}$ is the controller gain matrix. Then, the linear switching fuzzy controller can be described by

$$u(t) = \sum_{b=1}^{r} \psi_b(\varsigma(t_k)) K_b x(t_k) \tag{2.10}$$

for $t_k \leq t < t_{k+1}$. By integrating the controller (2.10) into the system (2.2), the following system is derived as follows:

$$\dot{x}(t) = \sum_{a=1}^{r}\sum_{b=1}^{r} \psi_a(\varsigma(t))\psi_b(\varsigma(t_k)) \left(A_a x(t) + B_a K_b x(t_k)\right) \tag{2.11}$$

for $t_k \leq t < t_{k+1}$.

Lemma 1. [14, 15] Let $w(\cdot) : [u, v] \to \mathbb{R}^n$ denote a continuous differential functions. For given scalars u, v and matrices $R \in \mathbb{S}_+^n$, $M_1, M_2 \in \mathbb{R}^{3n\times n}$, the following inequalities hold:

$$-\int_u^v w^T(s)Rw(s)ds \leq \rho^T(u, v)\Big((v-u)M_1R^{-1}M_1^T + \mathcal{M}_1(u, v)\Big)\rho(u, v), \tag{2.12}$$

$$-\int_u^v w^T(s)Rw(s)ds \leq \rho^T(u, v)\left((v-u)\mathcal{R} + \mathcal{M}_1(u, v) + \mathcal{M}_2(u, v)\right)\rho(u, v), \tag{2.13}$$

where $\mathcal{R} = M_1R^{-1}M_1^T + \frac{(v-u)^2}{3}M_2R^{-1}M_2^T$, $\mathcal{M}_1(u, v) = -Sym\{M_1[I_n, -I_n, 0_n]\}$, $\mathcal{M}_2(u, v) = -Sym\{M_2[I_n, I_n, -2I_n]\}$ and $\rho(u, v) = \left[w^T(v), w^T(u), \frac{1}{v-u}\int_u^v w^T(s)ds\right]^T$.

3. Main results

In this section, the fuzzy-based sampled-data control problem of the system (2.11) is investigated by using the linear switching method. First, the stability criterion for the system (2.11) is discussed. Based on the first result, the controller design with input saturation is discussed.

For simplicity, block entry matrices are defined as follows: $\wp_i = [0_{n\times(i-1)n}, I_n, 0_{n\times(5-i)n}]^T \in \mathbb{R}^{5n\times n}$ $(i = 1, \cdots, 5)$, along with the subsequent notations:

$$\begin{aligned}
\eta_k &= t - t_k,\ \eta_{k+1} = t_{k+1} - t,\\
\zeta^T(t) &= \left[x^T(t), x^T(t_k), x^T(t_{k+1}), \dot{x}^T(t), \frac{1}{t-t_k}\int_{t_k}^{t} x^T(s)ds\right],\\
\Pi_1 &= [\wp_1 - \wp_2],\ \Pi_2 = [\wp_1 - \wp_3],\\
\Xi_{1[a]} &= Sym\left\{\wp_1 P_a \wp_4^T\right\},\\
\Xi_{21} &= \wp_2 U \wp_2^T,\ \Xi_{22} = -\wp_2 U \wp_2^T,\\
\Xi_3 &= Sym\left\{[-\Pi_1, \Pi_2]\left(R_1[\Pi_1, \Pi_2]^T + R_2[\wp_2, \wp_3]^T\right)\right\},\\
\Xi_{31} &= Sym\left\{[\wp_4, \wp_0]\left(R_1[\Pi_1, \Pi_2]^T + R_2[\wp_2, \wp_3]^T\right) + [\Pi_1, \wp_0]R_1[\wp_4, \wp_4]^T\right\},\\
\Xi_{32} &= Sym\left\{[\wp_0, \wp_4]\left(R_1[\Pi_1, \Pi_2]^T + R_2[\wp_2, \wp_3]^T\right) + [\wp_0, \Pi_2]R_1[\wp_4, \wp_4]^T\right\},\\
\Xi_4 &= -Sym\left\{\Pi_2 G_2 \wp_2^T + [\wp_4 - \wp_1]G_5\wp_4^T\right\},\\
\Xi_{41} &= [\wp_4, \wp_2]\begin{bmatrix} G_1 & G_2 \\ * & G_3\end{bmatrix}[\wp_4, \wp_2]^T - \wp_3 G_6 \wp_3^T,\\
\Xi_{42} &= [\wp_4, \wp_3]\begin{bmatrix} G_4 & G_5 \\ * & G_6\end{bmatrix}[\wp_4, \wp_3]^T - \wp_2 G_3 \wp_2^T,\\
\Xi_{5[a,b]} &= -Sym\left\{\Pi_1 Y_{1[a,b]} + 3[\wp_1 + \wp_2 - 2\wp_5]Y_{2[a,b]} - \Pi_2 Y_{3[a,b]}\right\},\\
\Xi_{6[a,b]} &= Sym\left\{(\wp_1 X_1 + \wp_4 X_2)\left(-\wp_4^T + A_a\wp_1^T + B_a K_b \wp_2^T\right)\right\},\\
\Phi_{1[a,b]} &= \Xi_{1[a]} + \Xi_3 + \Xi_4 + \Xi_{5[a,b]} + \Xi_{6[a,b]},\\
\Phi_2 &= \Xi_{21} + \Xi_{31} + \Xi_{41},\ \Phi_3 = \Xi_{22} + \Xi_{32} + \Xi_{42}.
\end{aligned} \tag{3.1}$$

Theorem 1. For given matrices $K_b \in \mathbb{R}^{m\times n}$ and scalars $h_M > 0$, if the matrices $P_a, G_1, G_3, G_4, G_6 \in \mathbb{S}_+^n$, $U, X_1, X_2 \in \mathbb{S}^n$, $R_1, R_2, G_2, G_5 \in \mathbb{R}^{n\times n}$ and $Y_{1[a,b]}, Y_{2[a,b]}, Y_{3[a,b]} \in \mathbb{R}^{m\times n}$ satisfy the following LMIs:

$$\dot{P}_h \leq 0, \tag{3.2}$$

$$\begin{bmatrix} \Phi_{1[a,b]} + h_M\Phi_2 & h_M Y_{3[a,b]}^T \\ * & -h_M G_4\end{bmatrix} < 0, \tag{3.3}$$

$$\begin{bmatrix} \Phi_{1[a,b]} + h_M\Phi_3 & h_M[Y_{1[a,b]}, Y_{2[a,b]}]^T \\ * & -h_M diag\{G_1, 3G_1\}\end{bmatrix} < 0 \tag{3.4}$$

for all $a, b = 1, \cdots, r$, then the system (2.11) is asymptotically stable.

Proof. Let us choose the following Lyapunov functional and looped-functional candidate:

$$V(t) = \sum_{i=1}^{4} V_i(t), \tag{3.5}$$

where

$$\begin{aligned}
V_1(t) &= x^T(t)P_h x(t),\\
V_2(t) &= \eta_{k+1}\eta_k x^T(t_k)Ux(t_k),\\
V_3(t) &= 2\begin{bmatrix}\eta_{k+1}(x(t)-x(t_k))\\ \eta_k(x(t)-x(t_{k+1}))\end{bmatrix}^T\left(R_1\begin{bmatrix}x(t)-x(t_k)\\ x(t)-x(t_{k+1})\end{bmatrix}+R_2\phi_1(t_k,t_{k+1})\right),\\
V_4(t) &= \eta_{k+1}\int_{t_k}^{t}\phi_2(s,t_k)^T\begin{bmatrix}G_1 & G_2\\ * & G_3\end{bmatrix}\phi_2(s,t_k)ds-\eta_k\int_{t}^{t_{k+1}}\phi_2(s,t_{k+1})^T\begin{bmatrix}G_4 & G_5\\ * & G_6\end{bmatrix}\phi_2(s,t_{k+1})ds.
\end{aligned}$$

Here, the vectors $\phi_1(\alpha,\beta)$ and $\phi_2(\alpha,\beta)$ are respectively defined as

$$\phi_1(\alpha,\beta)=\left[x^T(\alpha),x^T(\beta)\right]^T,\ \phi_2(\alpha,\beta)=\left[\dot{x}^T(\alpha),x^T(\beta)\right]^T.$$

Calculating the time derivatives of $V_i(t)\,(i=1,\cdots,4)$ leads to

$$\begin{aligned}
\dot{V}_1(t) &= 2x^T(t)P_h\dot{x}(t)+x^T(t)\dot{P}_h x(t)\\
&= \sum_{a=1}^{r}\psi_a(\varsigma(t))\zeta^T(t)\Xi_{1[a]}\zeta(t)+x^T(t)\dot{P}_h x(t), \qquad (3.6)\\
\dot{V}_2(t) &= -\eta_k x^T(t_k)Ux(t_k)+\eta_{k+1}x^T(t_k)Ux(t_k)\\
&= \zeta^T(t)\left(\eta_{k+1}\Xi_{21}+\eta_k\Xi_{22}\right)\zeta(t), \qquad (3.7)\\
\dot{V}_3(t) &= 2\begin{bmatrix}-(x(t)-x(t_k))+\eta_{k+1}\dot{x}(t)\\ (x(t)-x(t_{k+1}))+\eta_k\dot{x}(t)\end{bmatrix}^T\left(R_1\begin{bmatrix}x(t)-x(t_k)\\ x(t)-x(x_{k+1})\end{bmatrix}+R_2\phi_1(t_k,t_{k+1})\right)\\
&\quad +2\begin{bmatrix}\eta_{k+1}(x(t)-x(t_k))\\ \eta_k(x(t)-x(t_{k+1}))\end{bmatrix}^T R_1\dot{\phi}_1(t,t)\\
&= \zeta^T(t)\left(\Xi_3+\eta_{k+1}\Xi_{31}+\eta_k\Xi_{32}\right)\zeta(t), \qquad (3.8)\\
\dot{V}_4(t) &= -\int_{t_k}^{t}\phi_2(s,t_k)^T\begin{bmatrix}G_1 & G_2\\ * & G_3\end{bmatrix}\phi_2(s,t_k)ds-\int_{t}^{t_{k+1}}\phi_2(s,t_{k+1})^T\begin{bmatrix}G_4 & G_5\\ * & G_6\end{bmatrix}\phi_2(s,t_{k+1})ds\\
&\quad +\eta_{k+1}\phi_2(t,t_k)^T\begin{bmatrix}G_1 & G_2\\ * & G_3\end{bmatrix}\phi_2(t,t_k)+\eta_k\phi_2(t,t_{k+1})^T\begin{bmatrix}G_4 & G_5\\ * & G_6\end{bmatrix}\phi_2(t,t_{k+1})\\
&= \zeta^T(t)\left(\Xi_4+\eta_{k+1}\Xi_{41}+\eta_k\Xi_{42}\right)\zeta(t)\\
&\quad -\int_{t_k}^{t}\dot{x}^T(s)G_1\dot{x}(s)ds-\int_{t}^{t_{k+1}}\dot{x}^T(s)G_4\dot{x}(s)ds. \qquad (3.9)
\end{aligned}$$

By applying Lemma 1 for any matrices $Y_{1[a,b]}$, $Y_{2[a,b]}$ and $Y_{3[a,b]}$, the upper bounds of the integral terms in (3.9) can be estimated as follows:

$$\begin{aligned}
-\int_{t_k}^{t}\dot{x}^T(s)G_1\dot{x}(s)ds &\le \sum_{a=1}^{r}\sum_{b=1}^{r}\psi_a(\varsigma(t))\psi_b(\varsigma(t_k))\zeta^T(t)\left(-Sym\left\{\Pi_1 Y_{1[a,b]}+3[\wp_1+\wp_2-2\wp_5]Y_{2[a,b]}\right\}\right.\\
&\quad \left.+\eta_k Y_{1[a,b]}^T G_1^{-1}Y_{1[a,b]}+\eta_k Y_{2[a,b]}^T G_1^{-1}Y_{2[a,b]}\right)\zeta(t), \qquad (3.10)
\end{aligned}$$

$$-\int_t^{t_{k+1}} \dot{x}^T(s)G_4\dot{x}(s)ds \leq \sum_{a=1}^{r}\sum_{b=1}^{r}\psi_a(\varsigma(t))\psi_b(\varsigma(t_k))\zeta^T(t)\left(-Sym\{-\Pi_2 Y_{3[a,b]}\}\right.$$
$$\left.+\eta_{k+1}Y_{3[a,b]}^T G_4^{-1}Y_{3[a,b]}\right)\zeta(t). \tag{3.11}$$

Thus, from (3.9)–(3.11), $\dot{V}_4(t)$ has the following bound:

$$\dot{V}_4(t) \leq \sum_{a=1}^{r}\sum_{b=1}^{r}\psi_a(\varsigma(t))\psi_b(\varsigma(t_k))\zeta^T(t)\left(\Xi_4+\eta_{k+1}\Xi_{41}+\eta_k\Xi_{42}+\Xi_{5[a,b]}+\eta_k Y_{1[a,b]}^T G_1^{-1}Y_{1[a,b]}\right.$$
$$\left.+\eta_k Y_{2[a,b]}^T G_1^{-1}Y_{2[a,b]}+\eta_{k+1}Y_{3[a,b]}^T G_4^{-1}Y_{3[a,b]}\right)\zeta(t). \tag{3.12}$$

From the system (2.11), for any free-weighting matrices $X_1, X_2 \in \mathbb{S}^n$, the following equation holds:

$$0 = 2\sum_{a=1}^{r}\sum_{b=1}^{r}\psi_a(\varsigma(t))\psi_b(\varsigma(t_k))\left(x^T(t)X_1+\dot{x}^T(t)X_2\right)\left(A_a x(t)+B_a K_b x(t_k)-\dot{x}(t)\right)$$
$$= \sum_{a=1}^{r}\sum_{b=1}^{r}\psi_a(\varsigma(t))\psi_b(\varsigma(t_k))\zeta^T(t)\Xi_{6[a,b]}\zeta(t). \tag{3.13}$$

Considering the constraint in (3.2), and by combining (3.6)–(3.13), the derivative of $V(t)$ can be estimated as

$$\dot{V}(t) \leq \sum_{a=1}^{r}\sum_{b=1}^{r}\psi_a(\varsigma(t))\psi_b(\varsigma(t_k))\zeta^T(t)\left(\Xi_{1[a]}+\Xi_3+\Xi_4+\Xi_{5[a,b]}+\Xi_{6[a,b]}\right.$$
$$+\eta_{k+1}\left(\Xi_{31}+\Xi_{41}+Y_{3[a,b]}^T G_4^{-1}Y_{3[a,b]}\right)$$
$$\left.+\eta_k\left(\Xi_{32}+\Xi_{42}+Y_{1[a,b]}^T G_1^{-1}Y_{1[a,b]}+\eta_k Y_{2[a,b]}^T G_1^{-1}Y_{2[a,b]}\right)\right)\zeta(t)$$
$$= \sum_{a=1}^{r}\sum_{b=1}^{r}\psi_a(\varsigma(t))\psi_b(\varsigma(t_k))\zeta^T(t)\left(\frac{\eta_{k+1}}{h_k}\left(\Phi_{1[a,b]}+h_k\Phi_2+h_k Y_{3[a,b]}^T G_4^{-1}Y_{3[a,b]}\right)\right.$$
$$\left.+\frac{\eta_k}{h_k}\left(\Phi_{1[a,b]}+h_k\Phi_3+h_k Y_{1[a,b]}^T G_1^{-1}Y_{1[a,b]}+h_k Y_{2[a,b]}^T G_1^{-1}Y_{2[a,b]}\right)\right)\zeta(t). \tag{3.14}$$

The inequality (3.14) is dependent on t and h_k. So, the inequality (3.14) is equivalent as follows:

$$\Phi_{1[a,b]}+h_M\Phi_2+h_M Y_{3[a,b]}^T G_4^{-1}Y_{3[a,b]} < 0, \tag{3.15}$$
$$\Phi_{1[a,b]}+h_M\Phi_3+h_M Y_{1[a,b]}^T G_1^{-1}Y_{1[a,b]}+h_M Y_{2[a,b]}^T G_1^{-1}Y_{2[a,b]} < 0. \tag{3.16}$$

By the Schur complement, the inequalities (3.15) and (3.16) can be further expressed as (3.3) and (3.4), respectively. Therefore, if LMIs (3.2)–(3.4) are satisfied, the derivative of $V(t)$ can be guaranteed to be negative. Furthermore, in accordance with Theorem 1, the system (2.11) is asymptotically stable. This completes the proof. □

Remark 1. Theorem 1 provides the stability condition for T-S fuzzy sampled-data systems. Although looped-functionals $V_2(t)$ to $V_4(t)$ lead to more conservative results than recent studies, it has been

designed as (3.5) for application in actual systems.

Remark 2. Actuator saturation exists in most real-world systems. In particular, the control performance is significantly degraded by the nonlinear behavior of actuator saturation. Therefore, in this paper, the input saturation problem is solved by using a method described in [33], and the set, accordingly, is as follows:

Ellipsoid $\Upsilon(P,\sigma)$: Let $P \in \mathbb{R}^{n\times n}$ and $\sigma > 0$. Then, denote $\Upsilon(P,\sigma) = \left\{x(t) \in \mathbb{R}^n : x^T(t)Px(t) \leq \sigma\right\}$.

Polyhedral $\Theta(H_i)$: Let $H_i \in \mathbb{R}^{m\times n}$ be a matrix, χ be a positive scalar and $c_{i,k}$ be the kth row of the matrix H_i. Then, define $\Theta(H_i) = \{x(t) \in \mathbb{R}^n \,||c_{i,l}x(t)| \leq \chi, l = 1,\cdots,m\}$.

If $\Upsilon(P,\sigma) \subseteq \Theta(H_b)$, $b = 1,\cdots,r$, then the representation for the saturated control input is

$$sat(u(t)) = \sum_{b=1}^{r} \psi_b(x(t_k))\mathbb{K}_b x(t_k), \qquad t \in [t_k, t_{k+1}), \tag{3.17}$$

where $\mathbb{K}_b = \sum_{s=1}^{2^m} \eta_s \left[D_s K_b + (I - D_s)H_b\right]$ with $0 \leq \eta_s \leq 1$ and $\sum_{s=1}^{2_m} \eta_s = 1$. And, $sat\,(u(t)) = [sat(u_1(t)),\cdots,sat(u_m(t))]^T$ with $sat(u_q(t)) = sgn(u_q(t))min\left\{|u_q(t)|,\chi\right\}$, where $\chi > 0$ is a saturation limit.

If the switching rule given by (2.8) is utilized to establish stabilization conditions, for different S_p and C_p, $p = 1,\cdots,2^{r-1}$, the corresponding controller is given by

$$sat(u_p(t)) \;=\; \sum_{b=1}^{r} \psi_b(\varsigma(t_k))\mathbb{K}_{p,b} x(t_k), \qquad t \in [t_k, t_{k+1}), \tag{3.18}$$

where $\mathbb{K}_{p,b}$ represents the control gain parameters corresponding to each case. Then, for $t_k \leq t < t_{k+1}$, the controller becomes the switching controller described below:

$$sat(u(t)) : \begin{cases} sat(u_1(t)) = \sum_{b=1}^{r} \psi_b(\varsigma(t_k))\mathbb{K}_{1,b} x(t_k) \text{ for } S_1, \\ \qquad\qquad \vdots \\ sat(u_p(t)) = \sum_{b=1}^{r} \psi_b(\varsigma(t_k))\mathbb{K}_{p,b} x(t_k) \text{ for } S_p. \end{cases} \tag{3.19}$$

Using (3.17) and (3.19), closed-loop systems can be formulated as

$$\dot{x}(t) = \sum_{a=1}^{r}\sum_{b=1}^{r} \psi_a(\varsigma(t))\psi_b(\varsigma(t_k))\left(A_a x(t) + B_a \mathbb{K}_{p,b} x(t_k)\right) \tag{3.20}$$

for $t_k \leq t < t_{k+1}$.

Based on Theorem 1, the linear switching fuzzy-based sampled-data controller design for system (3.20) is derived. The notations are defined as follows:

$$\begin{aligned} \hat{P}_a &= XP_aX, \\ \hat{G}_1 &= XG_1X,\ \hat{G}_2 = XG_2X,\ \hat{G}_3 = XG_3X,\ \hat{G}_4 = XG_4X,\ \hat{G}_5 = XG_5X,\ \hat{G}_6 = XG_6X, \\ \hat{U} &= XUX,\ \hat{R}_1 = XR_1X,\ \hat{R}_2 = XR_2X, \\ \hat{Y}_{1[a,b]} &= XY_{1[a,b]}X,\ \hat{Y}_{2[a,b]} = XY_{2[a,b]}X,\ \hat{Y}_{3[a,b]} = XY_{3[a,b]}X, \\ \mathbb{X}_5 &= diag\,\{X,X,X,X,X\}, \end{aligned}$$

$$
\begin{aligned}
\hat{\Xi}_{1[a]} &= \mathbb{X}_5\Xi_{1[a]}\mathbb{X}_5,\ \hat{\Xi}_{21} = \mathbb{X}_5\Xi_{21}\mathbb{X}_5,\ \hat{\Xi}_{22} = \mathbb{X}_5\Xi_{22}\mathbb{X}_5,\ \hat{\Xi}_3 = \mathbb{X}_5\Xi_3\mathbb{X}_5,\\
\hat{\Xi}_{31} &= \mathbb{X}_5\Xi_{31}\mathbb{X}_5,\ \hat{\Xi}_{32} = \mathbb{X}_5\Xi_{32}\mathbb{X}_5,\ \hat{\Xi}_4 = \mathbb{X}_5\Xi_4\mathbb{X}_5,\ \hat{\Xi}_5 = \mathbb{X}_5\Xi_5\mathbb{X}_5,\\
\mathbb{V}_{[p,b]} &= \sum_{s=1}^{2^m}\eta_s\left[D_sV_{p,b} + (I_m - D_s)N_{p,b}\right],\\
\hat{\Xi}_{6[a,b]} &= Sym\left\{(\wp_1 + \alpha\wp_4)\left(-X\wp_4^T + A_aX\wp_1^T + B_a\mathbb{V}_{p,b}\wp_2^T\right)\right\},\\
\hat{\Phi}_{1[a,b]} &= \hat{\Xi}_{1[a]} + \hat{\Xi}_3 + \hat{\Xi}_4 + \hat{\Xi}_5 + \hat{\Xi}_{5[a,b]} + \hat{\Xi}_{6[a,b]},\\
\hat{\Phi}_2 &= \hat{\Xi}_{21} + \hat{\Xi}_{31} + \hat{\Xi}_{41},\\
\hat{\Phi}_3 &= \hat{\Xi}_{22} + \hat{\Xi}_{32} + \hat{\Xi}_{42},\ (a,b = 1,\cdots,r).
\end{aligned}
\tag{3.21}
$$

Theorem 2. Let us assume that $\Upsilon(P_a,\sigma) \subset \Theta(H_b)$. For the given positive scalars h_M, α, χ, σ, η_s $(s = 1,2,\cdots,2^m)$ and matrices Q and R, if the matrices $\hat{P}_a, \hat{G}_1, \hat{G}_3, \hat{G}_4, \hat{G}_6 \in \mathbb{S}_+^n$, $\hat{U}, X \in \mathbb{S}^n$, $\hat{R}_1, \hat{R}_2, \hat{G}_2, \hat{G}_5 \in \mathbb{R}^{n\times n}$, $V_{p,b}, N_{p,b} \in \mathbb{R}^{m\times n}$ and $\hat{Y}_{1[a,b]}, \hat{Y}_{2[a,b]}, \hat{Y}_{3[a,b]} \in \mathbb{R}^{m\times n}$ satisfy the following LMIs:

$$
\dot{\hat{P}}_h \le 0, \tag{3.22}
$$

$$
\begin{bmatrix}
\hat{\Phi}_{1[a,b]} + h_M\hat{\Phi}_2 & h_M\hat{Y}_{3[a,b]}^T & \wp_1X & \wp_2V_{p,b}^T\\
* & -\hat{G}_2 & 0_{n\times n} & 0_{n\times m}\\
* & * & -Q^{-1} & 0_{n\times m}\\
* & * & * & -R^{-1}
\end{bmatrix} < 0, \tag{3.23}
$$

$$
\begin{bmatrix}
\hat{\Phi}_{1[a,b]} + h_M\hat{\Phi}_3 & h_M[\hat{Y}_{1[a,b]}, \hat{Y}_{2[a,b]}]^T & \wp_1X & \wp_2V_{p,b}^T\\
* & -diag\{\hat{G}_1, 3\hat{G}_1\} & 0_{n\times n} & 0_{n\times m}\\
* & * & -Q^{-1} & 0_{n\times m}\\
* & * & * & -R^{-1}
\end{bmatrix} < 0, \tag{3.24}
$$

$$
\begin{bmatrix}
\frac{1}{\sigma} & \frac{n_{p,b,k}}{\chi}\\
* & \hat{P}_a
\end{bmatrix} \ge 0 \tag{3.25}
$$

for all $a,b = 1,\cdots,r$ and $k = 1,\cdots,m$, then the system (3.20) is asymptotically stabilized. Here, $n_{p,b,k}$ is the kth row of the matrix $N_{p,b}$. And, the controller gain matrices are given by $K_{p,b} = V_{p,b}X^{-1}$.

Proof. By combining (3.14) and the cost function $J = \int_0^\infty \left[x^T(t)Qx(t) + u^T(t)Ru(t)\right]dt$ derived from the linear-quadratic regulator (LQR) technique, an upper bound of $\dot{V}(t)$ can be given by

$$
\begin{aligned}
\dot{V}(t) &\le \sum_{a=1}^{r}\sum_{b=1}^{r}\psi_a(\varsigma(t))\psi_b(\varsigma(t_k))\zeta^T(t)\left(\frac{\eta_{k+1}}{h_k}\left(\Phi_{1[a,b]} + \Phi_2 + Y_{3[a,b]}^TG_2^{-1}Y_{3[a,b]}\right)\right.\\
&\qquad \left. + \frac{\eta_k}{h_k}\left(\Phi_{1[a,b]} + \Phi_3Y_{1[a,b]}^TG_1^{-1}Y_{1[a,b]} + Y_{2[a,b]}^TG_1^{-1}Y_{2[a,b]}\right)\right)\zeta(t)\\
&\le \sum_{a=1}^{r}\sum_{b=1}^{r}\psi_a(\varsigma(t))\psi_b(\varsigma(t_k))\zeta^T(t)\left(\frac{\eta_{k+1}}{h_k}\left(\Phi_{1[a,b]} + \Phi_2 + Y_{3[a,b]}^TG_2^{-1}Y_{3[a,b]}\right)\right.\\
&\qquad + \frac{\eta_k}{h_k}\left(\Phi_{1[a,b]} + \Phi_3Y_{1[a,b]}^TG_1^{-1}Y_{1[a,b]} + Y_{2[a,b]}^TG_1^{-1}Y_{2[a,b]}\right)\\
&\qquad \left. -\wp_1Q\wp_1^T - \wp_2K_{p,b}^TRK_{p,b}\wp_2^T\right)\zeta(t) < 0.
\end{aligned}
\tag{3.26}
$$

The inequality (3.26) is dependent on t and h_k as proof of Theorem 1. So, based on the Schur

complement, the inequality (3.26) is equivalent to

$$\begin{bmatrix} \Phi_{1[a,b]} + h_M\Phi_2 & h_M Y_{3[a,b]}^T & \wp_1 & \wp_2 K_{p,b}^T \\ * & -G_2 & 0_{n\times n} & 0_{n\times m} \\ * & * & -Q^{-1} & 0_{n\times m} \\ * & * & * & -R^{-1} \end{bmatrix} < 0, \tag{3.27}$$

$$\begin{bmatrix} \Phi_{1[a,b]} + h_M\Phi_3 & h_M[Y_{1[a,b]}, Y_{2[a,b]}]^T & \wp_1 & \wp_2 K_{p,b}^T \\ * & -diag\{G_1, 3G_1\} & 0_{n\times n} & 0_{n\times m} \\ * & * & -Q^{-1} & 0_{n\times m} \\ * & * & * & -R^{-1} \end{bmatrix} < 0. \tag{3.28}$$

Define $X = X_1^{-1}$, $X_2 = \alpha X_1$, $\mathbb{V}_{p,b} = \mathbb{K}_{p,b}X$ and the matrices $\mathbb{X}_q = diag\underbrace{\{X, \cdots, X\}}_{\textbf{q elements}}$. By pre- and post-multiplying the matrices (3.27) and (3.28) by $diag\{\mathbb{X}_6, I_n, I_m\}$ and $diag\{\mathbb{X}_7, I_n, I_m\}$, then the inequalities (3.27) and (3.28) are respectively equivalent to (3.23) and (3.24).

The saturated controller in (3.20) exists if $\Upsilon(P_a, \sigma) \subset \Theta(H_b)$ [33]; it can be equivalently written as

$$P_a \geq \frac{\sigma}{\chi^2} c_{p,b,k}^T c_{p,b,k}, \quad a, b = 1, \cdots, r,\ k = 1, \cdots, m. \tag{3.29}$$

By the Schur complement, the inequality (3.29) is equivalent to

$$\begin{bmatrix} \frac{1}{\sigma} & \frac{c_{p,b,k}}{\chi} \\ * & P_a \end{bmatrix} \geq 0. \tag{3.30}$$

The inequality (3.30), by pre- and post-multiplying it with $diag\{1, X\}$ can yield the inequality (3.25). This completes the proof. □

In order to show the effectiveness of the Lyapunov function and looped-funtionals, the following system without input saturation is considered:

$$\dot{x}(t) = \sum_{a=1}^{r}\sum_{b=1}^{r} \psi_a(\varsigma(t))\psi_b(\varsigma(t_k)) \left(A_a x(t) + B_a K_{p,b} x(t_k)\right). \tag{3.31}$$

Then, the following theorem can be obtained easily.

Corollary 1. For given positive scalars h_M, α and matrices Q and R, the system (3.31) is asymptotically stable if the matrices $\hat{P}_a, \hat{G}_1, \hat{G}_3, \hat{G}_4, \hat{G}_6 \in \mathbb{S}_+^n$, $\hat{U}, X \in \mathbb{S}^n$, $\hat{R}_1, \hat{R}_2, \hat{G}_2, \hat{G}_5 \in \mathbb{R}^{n\times n}$, $V_{p,b}, N_{p,b} \in \mathbb{R}^{m\times n}$ and $\hat{Y}_{1[a,b]}, \hat{Y}_{2[a,b]}, \hat{Y}_{3[a,b]} \in \mathbb{R}^{m\times n}$ satisfy LMI (3.22) and the following LMIs for all $a, b = 1, \cdots, r$:

$$\begin{bmatrix} \bar{\Phi}_{1[a,b]} + h_M\hat{\Phi}_2 & h_M \hat{Y}_{3[a,b]}^T & \wp_1 X & \wp_2 V_{p,b}^T \\ * & -\hat{G}_2 & 0_{n\times n} & 0_{n\times m} \\ * & * & -Q^{-1} & 0_{n\times m} \\ * & * & * & -R^{-1} \end{bmatrix} < 0, \tag{3.32}$$

$$\begin{bmatrix} \bar{\Phi}_{1[a,b]} + h_M\hat{\Phi}_3 & h_M[\hat{Y}_{1[a,b]}, \hat{Y}_{2[a,b]}]^T & \wp_1 X & \wp_2 V_{p,b}^T \\ * & -diag\{\hat{G}_1, 3\hat{G}_1\} & 0_{n\times n} & 0_{n\times m} \\ * & * & -Q^{-1} & 0_{n\times m} \\ * & * & * & -R^{-1} \end{bmatrix} < 0, \tag{3.33}$$

where

$$\begin{aligned}\bar{\Phi}_{1[a,b]} &= \hat{\Xi}_{1[a]} + \hat{\Xi}_3 + \hat{\Xi}_4 + \hat{\Xi}_5 + \hat{\Xi}_{5[a,b]} + \bar{\Xi}_{6[a,b]},\\ \bar{\Xi}_{6[a,b]} &= Sym\left\{(\wp_1 + \alpha\wp_4)\left(-X\wp_4^T + A_aX\wp_1^T + B_aV_{p,b}\wp_2^T\right)\right\}.\end{aligned}$$

And, the controller gain matrices are given by $K_{p,b} = V_{p,b}X^{-1}$.

4. Examples

In this section, there are two examples to show the superiority and effectiveness of the proposed results.

Example 1: Consider the following chaotic Lorenz system modeled as T-S fuzzy system (2.2):

$$A_1 = \begin{bmatrix} -a & a & 0 \\ c & -1 & -d \\ 0 & d & -b \end{bmatrix}, A_2 = \begin{bmatrix} -a & a & 0 \\ c & -1 & d \\ 0 & -d & -b \end{bmatrix}, B_1 = B_2 = \begin{bmatrix} 1 \\ 0 \\ 0 \end{bmatrix}. \tag{4.1}$$

The fuzzy membership functions are $\psi_1(x(t)) = (1/2)(1 + x_1(t)/d)$ and $\psi_2(x(t)) = 1 - \psi_1(x_1(t))$.

In this example, the following parameters are chosen as $a = 10, b = 8/3, c = 28, d = 25$, and the initial conditions are applied as $x(0) = [10, 5, -15]^T$. In Table 1, the maximum allowable sampling bound h_M is calculated by applying Theorem 2, and it is listed with the existing works. Here, the result is obtained for $h_M = 0.0442, \alpha = 0.012, Q = 1, R = diag\{1, 1, 1\}$. The corresponding control gains are given as

$$\begin{aligned}K_{1,1} &= [-31.9071, -26.9334, -0.2229], K_{1,2} = [-31.9071, -26.9334, -0.2229],\\ K_{2,1} &= [-31.8505, -26.9543, 0.1921], K_{2,2} = [-31.8505, -26.9543, 0.1921].\end{aligned} \tag{4.2}$$

Although simple looped-functionals are utilized in Corollary 1, unlike in [38], the use of a linear switching method in Corollary 1 leads to less conservative results, as presented in Table 1. Figure 1 (a),(b) respectively show the state and input trajectories of the system (3.31).

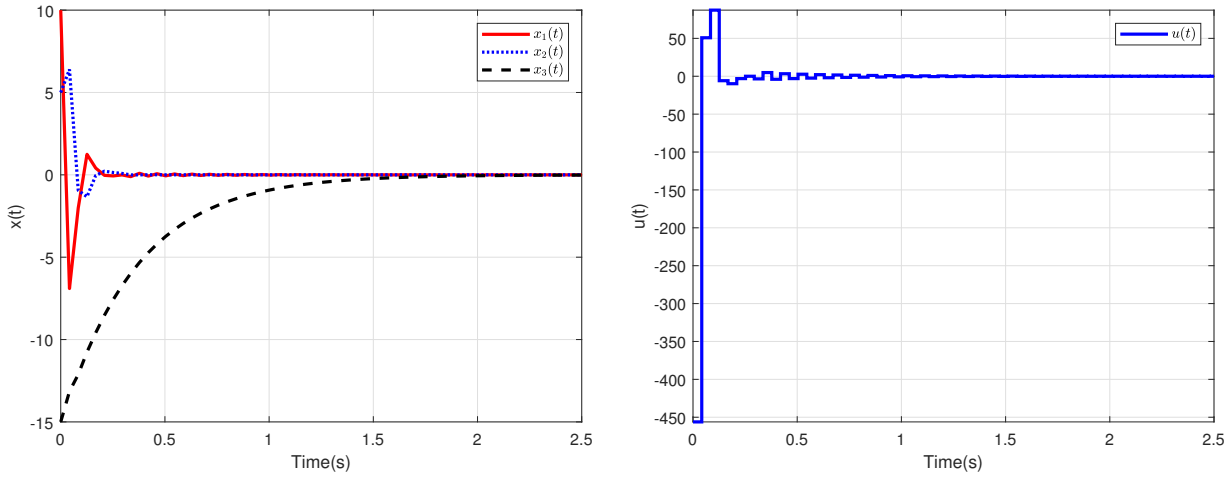

(a) Controlled state trajectories. **(b)** Control input trajectory

Figure 1. Controlled state and control input trajectories of the system (3.31).

Table 1. The maximum sampling bound h_M.

Method	[34]	[35]	[36]	[37]	[38]	Corollary 1
h_M	0.0158	0.0299	0.0347	0.0412	0.0438	0.0442

Example 2: The inverted pendulum, an under-actuated system, is often used as a benchmark for the performance of nonlinear control laws in control system theory due to its nonlinear behaviors, like gravity and centripetal force. For this reason, many papers have used examples modeled with a T-S fuzzy system [26, 27], and in this paper, a more complex model, the RIP system, is utilized.

Consider the following nonlinear RIP system of Figure 2:

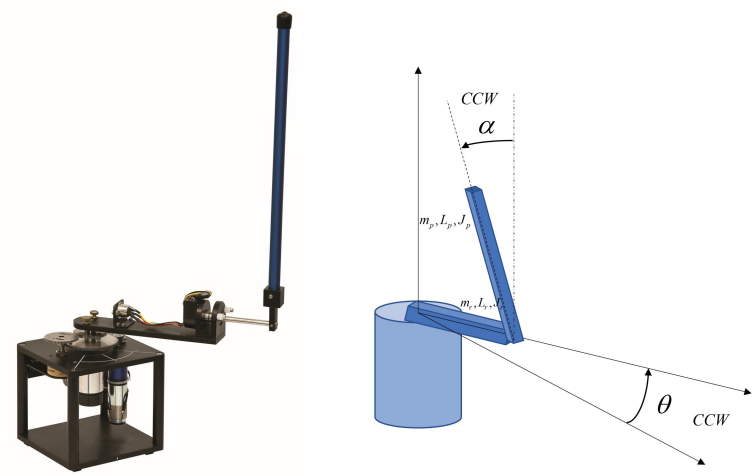

Figure 2. RIP from Quanser.

$$\left(m_pL_r^2+\frac{1}{4}m_pL_p^2-\frac{1}{4}m_pL_p^2cos^2(\alpha)+J_r\right)\ddot{\theta}-\left(\frac{1}{2}m_pL_pL_rcos(\alpha)\right)\ddot{\alpha}+\left(\frac{1}{2}m_pL_p^2sin(\alpha)cos(\alpha)\right)\dot{\theta}\dot{\alpha}$$
$$+\left(\frac{1}{2}m_pL_pL_rsin(\alpha)\right)\dot{\alpha}^2=\tau-B_r\dot{\theta}, \quad (4.3)$$

$$-\frac{1}{2}m_pL_pL_rcos(\alpha)\ddot{\theta}+\left(J_p+\frac{1}{4}m_pL_p^2\right)\ddot{\alpha}-\frac{1}{4}m_pL_p^2cos(\alpha)sin(\alpha)\dot{\theta}^2-\frac{1}{2}m_pL_pgsin(\alpha)=-B_p\dot{\alpha}. \quad (4.4)$$

In the system, $\theta(t)$ represents the angle of the rotary arm, $\dot{\theta}(t)$ signifies its angular velocity and $\alpha(t)$ and $\dot{\alpha}(t)$ depict the angle and angular velocity of the pendulum rod, respectively. The detailed definitions of the system parameters from (4.3) and (4.4) are shown in Table 2 and can be viewed in more detail in [39]. Additionally, the equation for torque, in terms of voltage, is as follows:

$$\tau(t)=\frac{\eta_gK_g\eta_mk_t\left(V_m(t)-K_gk_m\dot{\theta}\right)}{R_m}, \quad (4.5)$$

where $V_m(t)$ is the input servo motor voltage, subsequently being converted into $u(t)$. And, if $\dot{\alpha}(t)$ and $\dot{\theta}(t)$ are close to zero, the nonlinear Eqs (4.3) and (4.4) are expressed as follows:

$$\mathcal{F}\left(x(t)\right)\dot{x}(t)=\mathcal{A}\left(x(t)\right)x(t)+\mathcal{B}u(t), \quad (4.6)$$

where

$$
\begin{aligned}
x(t) &= [x_1(t), x_2(t), x_3(t), x_4(t)]^T = \left[\theta(t), \alpha(t), \dot{\theta}(t), \dot{\alpha}(t)\right]^T, \\
u(t) &= V_m(t), \\
\mathcal{F}(x(t)) &= \begin{bmatrix} 1 & 0 & 0 & 0 \\ 0 & 1 & 0 & 0 \\ 0 & 0 & \mathcal{F}_{33} & -\frac{1}{2}m_p L_p L_r cos(x_2(t)) \\ 0 & 0 & -\frac{1}{2}m_p L_p L_r cos(x_2(t)) & J_p + \frac{1}{4}m_p L_p^2 \end{bmatrix}, \\
\mathcal{A}(x(t)) &= \begin{bmatrix} 0 & 0 & 1 & 0 \\ 0 & 0 & 0 & 1 \\ 0 & 0 & -\frac{\eta_g \eta_m K_g^2 k_t k_m}{R_m} - B_r & 0 \\ 0 & \frac{1}{2}m_p L_p g sinc(x_2(t)) & 0 & -B_p \end{bmatrix}, \\
\mathcal{B} &= \begin{bmatrix} 0 \\ 0 \\ \frac{\eta_g \eta_m K_g k_t}{R_m} \\ 0 \end{bmatrix}, \\
\mathcal{F}_{33} &= m_p L_r^2 + \frac{1}{4}m_p L_p^2 - \frac{1}{4}m_p L_p^2 cos^2(x_2(t)) + J_r.
\end{aligned}
$$

By multiplying $\mathcal{F}^{-1}(x(t))$ to the Eq (4.6) and defining $\mathcal{F}^{-1}(x(t))\mathcal{A}(x(t)) = A(x(t))$ and $\mathcal{F}^{-1}(x(t))\mathcal{B} = B(x(t))$, system (2.2) can be derived.

Table 2. Physical parameters of the RIP.

Symbol	Value	Symbol	Value
L_p	0.337 $[m]$	L_r	0.216 $[m]$
k_t	0.00767 $[Nm/A]$	k_m	0.00767 $[Vs/rad]$
m_p	0.127 $[kg]$	R_m	2.6 $[\Omega]$
B_p	0.0024 $[Nms/rad]$	B_r	0.0024 $[Nms/rad]$
η_g	0.9	η_m	0.6
J_p	0.0012 $[kgm^2]$	J_r	0.000998 $[kgm^2]$
K_g	70	g	9.81 $[m/s^2]$

To formalize the T-S fuzzy model in Eq (4.6), the following two premise variables ($r = 2$) were selected, resulting in the utilization of 2^r IF-THEN rules:

$$\varsigma_1(t) = cos(x_2(t)), \varsigma_2(t) = sinc(x_2(t)). \tag{4.7}$$

When utilizing the local sector nonlinearity approach, it becomes possible to approximate nonlinear systems within the limitations of the fuzzy model. Therefore, the bounds of the premise variables described by (4.7) can be determined as follows by using $|\alpha| \leq \frac{\pi}{6}$ $[rad]$:

$$\varsigma_{1,max} = 1, \varsigma_{1,min} = 0.8660, \varsigma_{2,max} = 1, \varsigma_{2,min} = 0.6063. \tag{4.8}$$

Let us define

$$\begin{aligned} M_{11}(t) &= \frac{\varsigma_1(t) - \varsigma_{1,min}}{\varsigma_{1,max} - \varsigma_{1,min}}, M_{12}(t) = 1 - M_{11}(t), \\ M_{21}(t) &= \frac{\varsigma_2(t) - \varsigma_{2,min}}{\varsigma_{2,max} - \varsigma_{2,min}}, M_{22}(t) = 1 - M_{21}(t). \end{aligned} \tag{4.9}$$

Therefore, the membership functions can be calculated as

$$\begin{aligned} \vartheta_1(t) = M_{11}(t)M_{21}(t), \vartheta_2(t) = M_{12}(t)M_{21}(t), \\ \vartheta_3(t) = M_{11}(t)M_{22}(t), \vartheta_4(t) = M_{12}(t)M_{22}(t), \\ \psi_a(\varsigma(t)) = \frac{\vartheta_a(\varsigma(t))}{\Sigma_{b=1}^{r}\vartheta_b(\varsigma(t))}. \end{aligned} \tag{4.10}$$

And, this is shown in Figure 3 for $x_2(t)$.

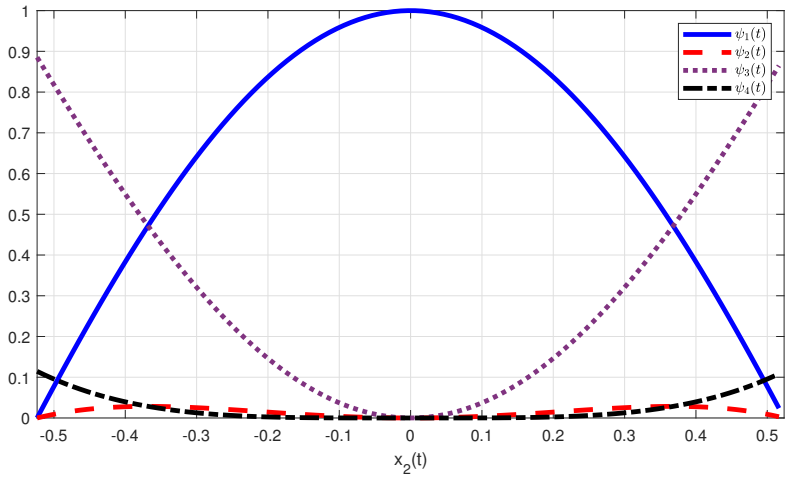

Figure 3. Membership function of RIP.

The matrices of system (2.2) according to the premise variables described by (4.7) and (4.8) and the parameters of Table 2 are as follows:

$$A_1 = \begin{bmatrix} 0 & 0 & 1 & 0 \\ 0 & 0 & 0 & 1 \\ 0 & 81.4085 & -25.1327 & -0.9317 \\ 0 & 121.9360 & -24.1728 & -1.3955 \end{bmatrix}, \quad A_2 = \begin{bmatrix} 0 & 0 & 1 & 0 \\ 0 & 0 & 0 & 1 \\ 0 & 38.9003 & -13.8672 & -0.4452 \\ 0 & 76.0390 & -11.5507 & -0.8702 \end{bmatrix},$$

$$A_3 = \begin{bmatrix} 0 & 0 & 1 & 0 \\ 0 & 0 & 0 & 1 \\ 0 & 49.3555 & -25.1327 & -0.9317 \\ 0 & 73.9262 & -24.1728 & -1.3955 \end{bmatrix}, \quad A_4 = \begin{bmatrix} 0 & 0 & 1 & 0 \\ 0 & 0 & 0 & 1 \\ 0 & 23.5841 & -13.8672 & -0.4452 \\ 0 & 46.1002 & -11.5507 & -0.8702 \end{bmatrix},$$

$$B_1 = B_2 = \begin{bmatrix} 0 \\ 0 \\ 45.0065 \\ 43.2876 \end{bmatrix}, \quad B_3 = B_4 = \begin{bmatrix} 0 \\ 0 \\ 24.8328 \\ 20.6846 \end{bmatrix}. \tag{4.11}$$

The experimental equipment shown in Figure 4 consists of a Quanser RIP, UPM-1503 voltage amplifier, q8 terminal board and SRV-02 plant. The Matlab/Simulink platform, as shown in Figure 5, is utilized to execute real-time controllers for the RIP. The Simulink file can be downloaded from [39], except for the internal controller blocks. The controller gain $K_{p,j}$ can be obtained by applying Theorem 2 using the sampling period $h_M = 0.01$, tuning parameters $\alpha = 0.47, \gamma = 5, \delta = 1, Q = diag\{5, 2, 1, 1\}, \eta_1 = \eta_2 = 0.5$ and $R = 0.1$; the results are listed in Table 3.

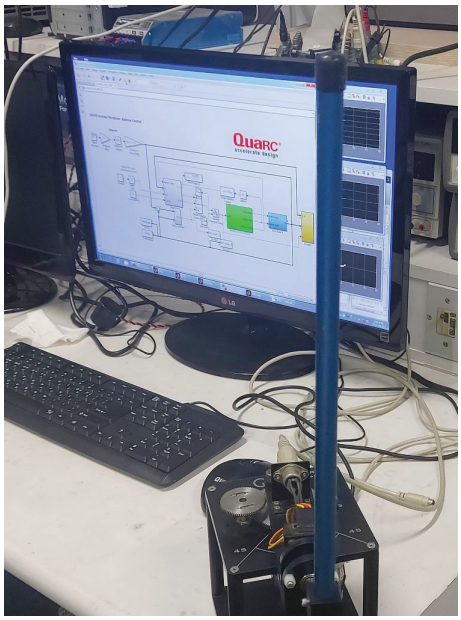

Figure 4. Experimental system for the RIP.

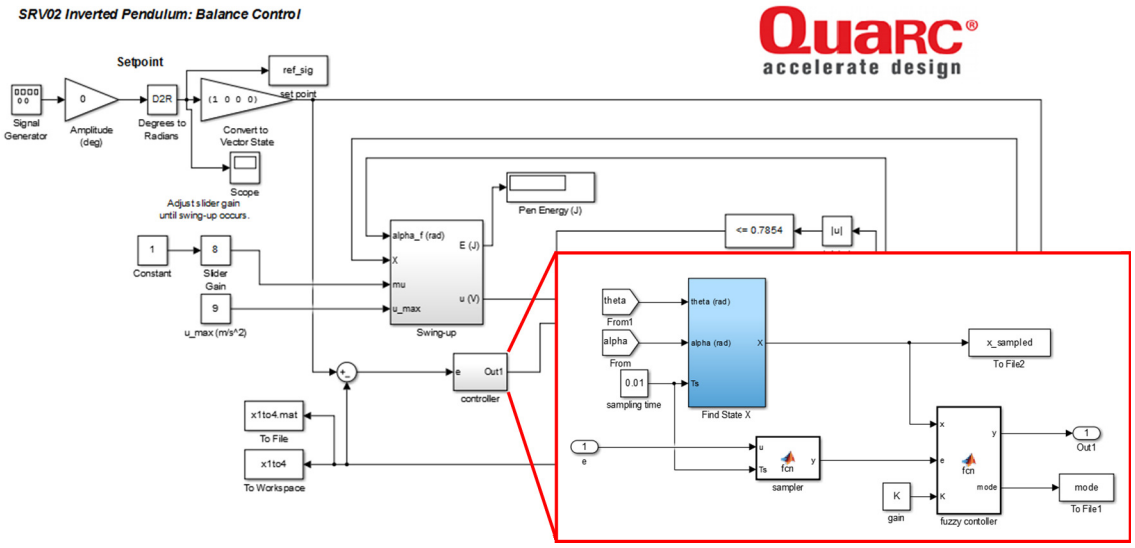

Figure 5. Matlab/Simulink program for RIP system with controller.

Table 3. The feedback gain.

Case	The feedback gain
1	$K_{1,1} = \begin{bmatrix} 0.8205 & -13.8725 & 1.6758 & -2.3288 \end{bmatrix}$
	$K_{1,2} = \begin{bmatrix} 0.8191 & -13.8626 & 1.6735 & -2.3265 \end{bmatrix}$
	$K_{1,3} = \begin{bmatrix} 0.8202 & -13.8679 & 1.6751 & -2.3280 \end{bmatrix}$
	$K_{1,4} = \begin{bmatrix} 0.8203 & -13.8687 & 1.6754 & -2.3282 \end{bmatrix}$
2	$K_{2,1} = \begin{bmatrix} 0.5321 & -9.2269 & 1.1086 & -1.5454 \end{bmatrix}$
	$K_{2,2} = \begin{bmatrix} 0.5325 & -9.2339 & 1.1094 & -1.5466 \end{bmatrix}$
	$K_{2,3} = \begin{bmatrix} 0.5326 & -9.2392 & 1.1095 & -1.5474 \end{bmatrix}$
	$K_{2,4} = \begin{bmatrix} 0.5331 & -9.2406 & 1.1105 & -1.5478 \end{bmatrix}$
3	$K_{3,1} = \begin{bmatrix} 0.4403 & -7.2309 & 0.8717 & -1.2275 \end{bmatrix}$
	$K_{3,2} = \begin{bmatrix} 0.4398 & -7.2218 & 0.8706 & -1.2256 \end{bmatrix}$
	$K_{3,3} = \begin{bmatrix} 0.4397 & -7.2200 & 0.8703 & -1.2254 \end{bmatrix}$
	$K_{3,4} = \begin{bmatrix} 0.4394 & -7.2140 & 0.8696 & -1.2243 \end{bmatrix}$
4	$K_{4,1} = \begin{bmatrix} 0.9552 & -17.1361 & 2.0117 & -2.8536 \end{bmatrix}$
	$K_{4,2} = \begin{bmatrix} 0.9547 & -17.1289 & 2.0109 & -2.8525 \end{bmatrix}$
	$K_{4,3} = \begin{bmatrix} 0.9544 & -17.1228 & 2.0100 & -2.8513 \end{bmatrix}$
	$K_{4,4} = \begin{bmatrix} 0.9550 & -17.1326 & 2.0113 & -2.8530 \end{bmatrix}$
5	$K_{5,1} = \begin{bmatrix} 1.6443 & -26.2578 & 3.2041 & -4.3896 \end{bmatrix}$
	$K_{5,2} = \begin{bmatrix} 1.6442 & -26.2566 & 3.2039 & -4.3894 \end{bmatrix}$
	$K_{5,3} = \begin{bmatrix} 1.6443 & -26.2589 & 3.2042 & -4.3898 \end{bmatrix}$
	$K_{5,4} = \begin{bmatrix} 1.6443 & -26.2579 & 3.2041 & -4.3896 \end{bmatrix}$
6	$K_{6,1} = \begin{bmatrix} 0.1379 & -1.1926 & 0.2263 & -0.2381 \end{bmatrix}$
	$K_{6,2} = \begin{bmatrix} 0.1378 & -1.1911 & 0.2260 & -0.2377 \end{bmatrix}$
	$K_{6,3} = \begin{bmatrix} 0.1376 & -1.1889 & 0.2257 & -0.2375 \end{bmatrix}$
	$K_{6,4} = \begin{bmatrix} 0.1379 & -1.1932 & 0.2263 & -0.2382 \end{bmatrix}$
7	$K_{7,1} = \begin{bmatrix} 0.9526 & -17.0428 & 1.9949 & -2.8525 \end{bmatrix}$
	$K_{7,2} = \begin{bmatrix} 0.9521 & -17.0316 & 1.9937 & -2.8505 \end{bmatrix}$
	$K_{7,3} = \begin{bmatrix} 0.9524 & -17.0382 & 1.9943 & -2.8517 \end{bmatrix}$
	$K_{7,4} = \begin{bmatrix} 0.9529 & -17.0462 & 1.9953 & -2.8530 \end{bmatrix}$
8	$K_{8,1} = \begin{bmatrix} 2.1742 & -36.1862 & 4.2889 & -6.0038 \end{bmatrix}$
	$K_{8,2} = \begin{bmatrix} 2.1737 & -36.1771 & 4.2880 & -6.0022 \end{bmatrix}$
	$K_{8,3} = \begin{bmatrix} 2.1736 & -36.1739 & 4.2875 & -6.0018 \end{bmatrix}$
	$K_{8,4} = \begin{bmatrix} 2.1732 & -36.1693 & 4.2870 & -6.0009 \end{bmatrix}$

When the state exceeds the bounds of the premise variable, an energy-based swing-up control is employed [40]. To compute $\dot{\theta}$ and $\dot{\alpha}$, a high-pass filter $F(s) = \frac{20\pi s}{s+20\pi}$ is utilized for the measured angle. The results obtained by applying the fuzzy switching controller using the gains in Table 3 are shown in Figures 6–8. In Figures 6 (a)–8 (a), energy-based swing-up control is performed for 0 to 3.34 seconds, and then stabilization is performed. And, Figures 6 (b)–8 (b) show stabilization when disturbance is introduced under the stable state. Figure 6 displays the angles and velocities of both the arm and rod through the results of $\theta(t)$, $\alpha(t)$, $\dot{\theta}(t)$ and $\dot{\alpha}(t)$. In addition, Figure 6 shows the stability when using the

control gain $K_{p,j}$ obtained via Theorem 2. Figure 7 displays the control input $u(t)$ signal, and it shows that the input saturation conditions are satisfied. Figure 8 depicts the case of the switching controller at that moment.

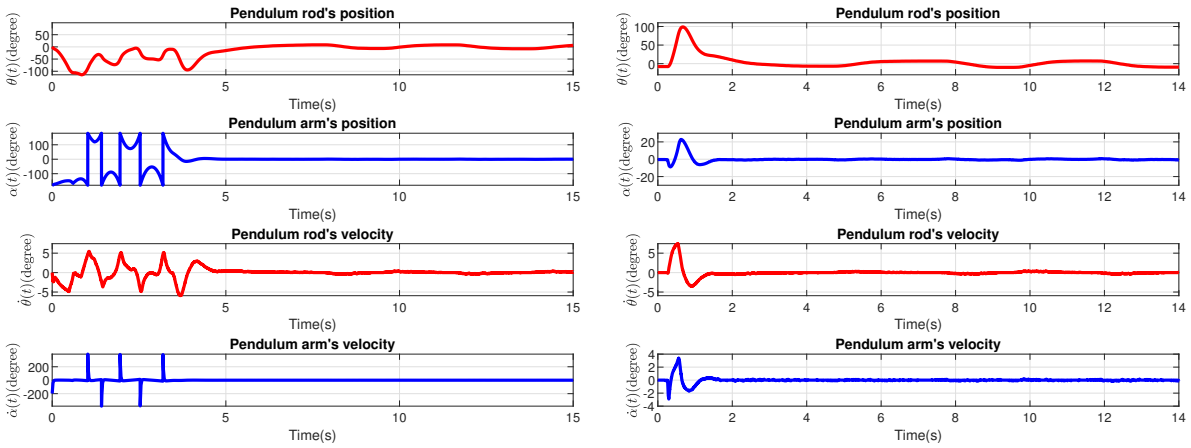

(a) Stabilization results with the swing-up control region. **(b)** Responses to a disturbance in the stable state.

Figure 6. Position and velocity responses of the RIP.

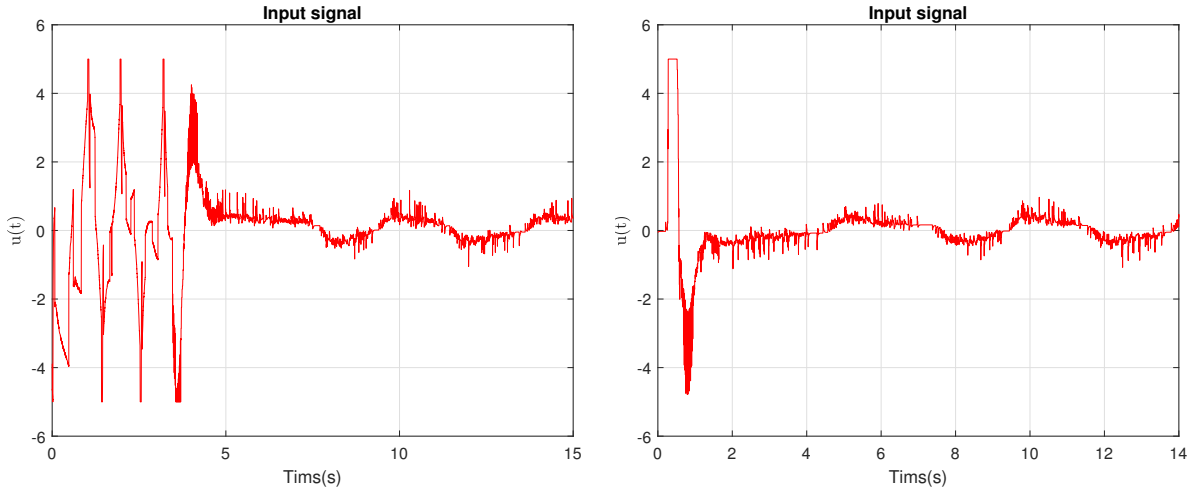

(a) Stabilization result with the swing-up control region. **(b)** Response to a disturbance in the stable state.

Figure 7. Input response of the RIP.

Remark 3. According to (4.10), there are four membership functions (ψ_1–ψ_4). Consequently, inspired by previous work [5], 2^{4-1} switching algorithms are derived by using ψ_1–ψ_3. However, the RIP system has only five cases: $S_1(\dot{\psi}_1 \leq 0,\ \dot{\psi}_2 \leq 0,\ \dot{\psi}_3 \leq 0)$, $S_2(\dot{\psi}_1 \leq 0,\ \dot{\psi}_2 \leq 0,\ \dot{\psi}_3 > 0)$, $S_4(\dot{\psi}_1 \leq 0,\ \dot{\psi}_2 > 0,\ \dot{\psi}_3 > 0)$, $S_5(\dot{\psi}_1 > 0,\ \dot{\psi}_2 \leq 0,\ \dot{\psi}_3 \leq 0)$ and $S_7(\dot{\psi}_1 > 0,\ \dot{\psi}_2 > 0,\ \dot{\psi}_3 \leq 0)$. S_1 is the unchanged situation, and S_2, S_4, S_5 and S_7 are shown from the right in Figure 9. Here, each boundary is $x_2 = -0.3636, 0$ and 0.3636 [rad]. As shown in Figure 8, five cases are presented; S_2 and S_7 are visible when $x_2(t)$ is larger than 0.3636 [rad], and S_1, S_4 and S_5 are frequently observed to be in a stable state.

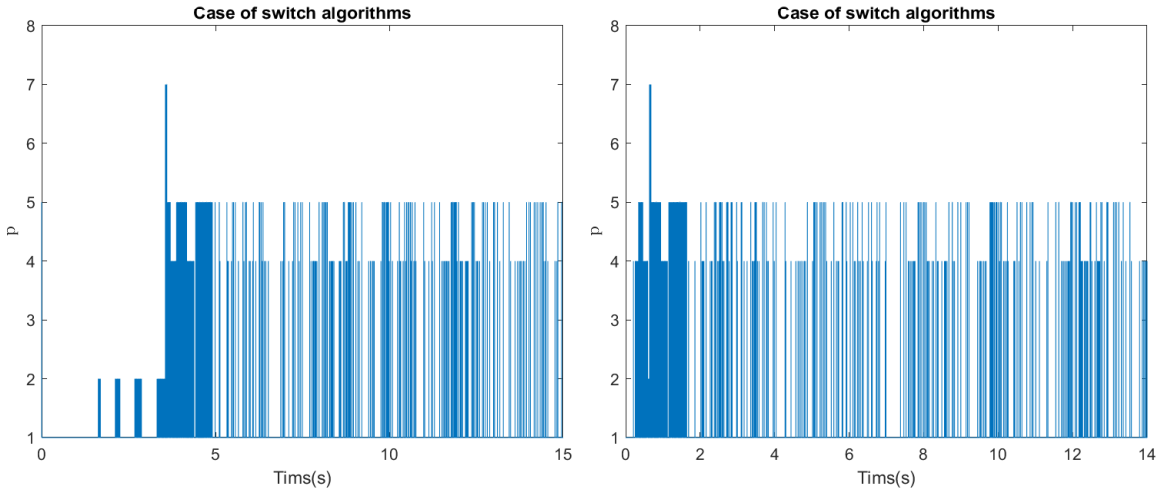

(a) Stabilization result with swing-up control region. **(b)** Response to a disturbance in the stable state.

Figure 8. Cases of switching of the RIP.

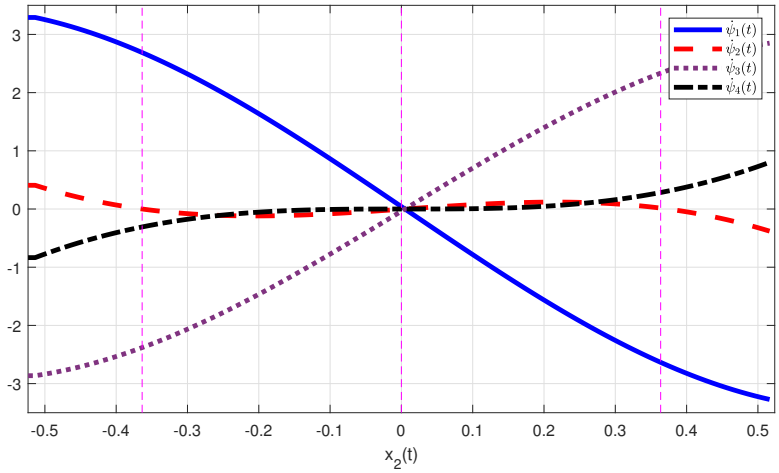

Figure 9. Derivative values of membership functions in the RIP.

5. Conclusions

In this paper, the fuzzy-based sampled-data control for the T-S fuzzy system with input saturation has been investigated. The linear switching method was employed to stabilize the fuzzy systems. By using the appropriate looped-functionals and some integral inequalities, the stability and stabilization criteria were obtained as the LMIs. Furthermore, the practical limitation of input saturation was considered for T-S fuzzy systems, and the LQR technique was employed for controller tuning. Moreover, the controller gain parameters were determined by solving the obtained set of LMIs. Finally, through the numerical example of the chaotic Lorenz model and the experiment of the RIP system, the excellence and effectiveness of the proposed results were confirmed, respectively. The numerical example showed that Corollary 1 was less conservative than previous results, and the experiments

confirmed that the stabilization of the RIP system was ensured when using the switching method. The future work will focus on improving the proposed design conservatism by taking into account more common phenomena, such as time-varying delays, uncertainties and external disturbances, and solving them using the active disturbance rejection control strategy and advanced integral inequality conditions. Additionally, the proposed sampled-data control design will be extended to event-triggered control in order to conserve communication resources.

Use of AI tools declaration

The authors declare they have not used Artificial Intelligence tools in the creation of this article.

Acknowledgments

This work was supported in part by the Basic Science Research Program through the National Research Foundation of Korea (NRF) funded by the Ministry of Education (Grant NRF-2022R1I1A1A01062831, NRF-2020R1A6A1A12047945 and NRF-2019R1I1A3A02058096), and under the Grand Information Technology Research Center Support Program supervised by the Institute for Information & Communications Technology Planning & Evaluation (IITP) under Grant IITP-2023-2020-0-01462. And, this work was also supported by Chungbuk National University BK21 program (2023).

Conflict of interest

The authors declare no conflict of interest.

References

1. T. Takagi, M. Sugeno, Fuzzy identification of systems and its applications to modeling and control, *IEEE T. Syst. Man Cy.*, **15** (1985), 116–132. http://dx.doi.org/10.1109/Tsmc.1985.6313399
2. Y. Liu, S. M. Lee, Stability and stabilization of Takagi-Sugeno fuzzy systems via sampled-data and state quantized controller, *IEEE T. Fuzzy Syst.*, **24** (2016), 635–644. http://dx.doi.org/10.1109/Tfuzz.2015.2469099
3. O. M. Kwon, M. J. Park, J. H. Park, S. M. Lee, Stability and stabilization of T-S fuzzy systems with time-varying delays via augmented Lyapunov-Krasovskii functionals, *Inform. Sci.*, **372** (2016), 1–15. http://dx.doi.org/10.1016/j.ins.2016.08.026
4. Y. J. Liu, J. H. Park, B. Z. Guo, Y. J. Shu, Further results on stabilization of chaotic systems based on fuzzy memory sampled-data control, *IEEE T. Fuzzy Syst.*, **26** (2018), 1040–1045. http://dx.doi.org/10.1109/Tfuzz.2017.2686364
5. L. K. Wang, H. K. Lam, A new approach to stability and stabilization analysis for continuous-time Takagi-Sugeno fuzzy systems with time delay, *IEEE T. Fuzzy Syst.*, **26** (2018), 2460–2465. http://dx.doi.org/10.1109/Tfuzz.2017.2752723

6. S. H. Lee, M. J. Park, O. M. Kwon, R. Sakthivel, A sampled-data control problem of neural-network-based systems using an improved free-matrix-based inequality, *J. Franklin I.*, **356** (2019), 8344–8365. http://dx.doi.org/10.1016/j.jfranklin.2019.08.001
7. C. Briat, A. Seuret, A looped-functional approach for robust stability analysis of linear impulsive systems, *Syst. Control Lett.*, **61** (2012), 980–988. http://dx.doi.org/10.1016/j.sysconle.2012.07.008
8. L. Hetel, J. Daafouz, S. Tarbouriech, C. Prieur, Stabilization of linear impulsive systems through a nearly-periodic reset, *Nonlinear Anal.-Hybri.*, **7** (2013), 4–15. http://dx.doi.org/10.1016/j.nahs.2012.06.001
9. E. Fridman, A. Seuret, J. P. Richard, Robust sampled-data stabilization of linear systems: An input delay approach, *Automatica*, **40** (2004), 1441–1446. http://dx.doi.org/10.1016/j.automatica.2004.03.003
10. P. Naghshtabrizi, J. P. Hespanha, A. R. Teel, Exponential stability of impulsive systems with application to uncertain sampled-data systems, *Syst. Control Lett.*, **57** (2008), 378–385. http://dx.doi.org/10.1016/j.sysconle.2007.10.009
11. E. Fridman, A refined input delay approach to sampled-data control, *Automatica*, **46** (2010), 421–427. http://dx.doi.org/10.1016/j.automatica.2009.11.017
12. K. Liu, E. Fridman, Wirtinger's inequality and Lyapunov-based sampled-data stabilization, *Automatica*, **48** (2012), 102–108. http://dx.doi.org/10.1016/j.automatica.2011.09.029
13. A. Seuret, A novel stability analysis of linear systems under asynchronous samplings, *Automatica*, **48** (2012), 177–182. http://dx.doi.org/10.1016/j.automatica.2011.09.033
14. A. Seuret, F. Gouaisbaut, Wirtinger-based integral inequality: Application to time-delay systems, *Automatica*, **49** (2013), 2860–2866. http://dx.doi.org/10.1016/j.automatica.2013.05.030
15. A. Seuret, C. Briat, Stability analysis of uncertain sampled-data systems with incremental delay using looped-functionals, *Automatica*, **55** (2015), 274–278. http://dx.doi.org/10.1016/j.automatica.2015.03.015
16. H. B. Zeng, J. H. Park, S. P. Xiao, Y. J. Liu, Further results on sampled-data control for master-slave synchronization of chaotic Lur'e systems with time delay, *Nonlinear Dynam.*, **82** (2015), 851–863. http://dx.doi.org/10.1007/s11071-015-2199-6
17. T. H. Lee, J. H. Park, Stability analysis of sampled-data systems via free-matrix-based time-dependent discontinuous Lyapunov approach, *IEEE T. Automat. Contr.*, **62** (2017), 3653–3657. http://dx.doi.org/10.1109/Tac.2017.2670786
18. H. B. Zeng, K. L. Teo, Y. He, A new looped-functional for stability analysis of sampled-data systems, *Automatica*, **82** (2017), 328–331. http://dx.doi.org/10.1016/j.automatica.2017.04.051
19. T. H. Lee, J. H. Park, Improved criteria for sampled-data synchronization of chaotic Lur'e systems using two new approaches, *Nonlinear Anal.-Hybri.*, **24** (2017), 132–145. http://dx.doi.org/10.1016/j.nahs.2016.11.006
20. T. Li, R. T. Yuan, S. M. Fei, Z. T. Ding, Sampled-data synchronization of chaotic lur'e systems via an adaptive event-triggered approach, *Inform. Sci.*, **462** (2018), 40–54. http://dx.doi.org/10.1016/j.ins.2018.06.012

21. N. Gunasekaran, G. S. Zhai, Q. Yu, Sampled-data synchronization of delayed multi-agent networks and its application to coupled circuit, *Neurocomputing*, **413** (2020), 499–511. http://dx.doi.org/10.1016/j.neucom.2020.05.060

22. K. Tanaka, T. Hori, H. O. Wang, A multiple Lyapunov function approach to stabilization of fuzzy control systems, *IEEE T. Fuzzy Syst.*, **11** (2003), 582–589. http://dx.doi.org/10.1109/Tfuzz.2003.814861

23. B. J. Rhee, S. Won, A new fuzzy Lyapunov function approach for a Takagi-Sugeno fuzzy control system design, *Fuzzy Set. Syst.*, **157** (2006), 1211–1228. http://dx.doi.org/10.1016/j.fss.2005.12.020

24. L. K. Wang, H. K. Lam, New stability criterion for continuous-time Takagi-Sugeno fuzzy systems with time-varying delay, *IEEE T. Cybernetics*, **49** (2019), 1551–1556. http://dx.doi.org/10.1109/Tcyb.2018.2801795

25. R. M. Zhang, D. Q. Zeng, J. H. Park, Y. J. Liu, S. M. Zhong, A new approach to stabilization of chaotic systems with nonfragile fuzzy proportional retarded sampled-data control, *IEEE T. Cybernetics*, **49** (2019), 3218–3229. http://dx.doi.org/10.1109/Tcyb.2018.2831782

26. J. R. Zhao, S. Y. Xu, J. H. Park, Improved criteria for the stabilization of T-S fuzzy systems with actuator failures via a sampled-data fuzzy controller, *Fuzzy Set. Syst.*, **392** (2020), 154–169. http://dx.doi.org/10.1016/j.fss.2019.09.004

27. L. Yang, J. Y. Zhang, C. Ge, W. Li, Z. W. Zhao, Stability and stabilization for uncertain fuzzy system with sampled-data control and state quantization, *Appl. Intell.*, **51** (2021), 7469–7483. http://dx.doi.org/10.1007/s10489-021-02206-8

28. Y. H. Zhang, H. Y. Li, J. Sun, W. He, Cooperative adaptive event-triggered control for multiagent systems with actuator failures, *IEEE T. Syst. Man Cy.*, **49** (2019), 1759–1768. http://dx.doi.org/10.1109/Tsmc.2018.2883907

29. Y. M. Li, J. X. Zhang, W. Liu, S. C. Tong, Observer-based adaptive optimized control for stochastic nonlinear systems with input and state constraints, *IEEE T. Neur. Net. Lear.*, **33** (2022), 7791–7805. http://dx.doi.org/10.1109/Tnnls.2021.3087796

30. L. K. Wang, H. K. Lam, J. H. Gu, Stability and stabilization for fuzzy systems with time delay by applying polynomial membership function and iteration algorithm, *IEEE T. Cybernetics*, **52** (2022), 11604–11613. http://dx.doi.org/10.1109/Tcyb.2021.3072797

31. H. B. Zeng, K. L. Teo, Y. He, W. Wang, Sampled-data stabilization of chaotic systems based on a T-S fuzzy model, *Inform. Sci.*, **483** (2019), 262–272. http://dx.doi.org/10.1016/j.ins.2019.01.046

32. P. Y. Tang, Y. C. Ma, Non-fragile sampled-date dissipative analysis for uncertain T-S fuzzy time delay system with actuator saturation, *ISA T.*, **106** (2020), 109–123. http://dx.doi.org/10.1016/j.isatra.2020.07.006

33. R. Sakthivel, R. Sakthivel, O. M. Kwon, P. Selvaraj, Disturbance rejection for singular semi-markov jump neural networks with input saturation, *Appl. Math. Comput.*, **407** (2021), 126301. http://dx.doi.org/10.1016/j.amc.2021.126301

34. H. K. Lam, F. H. F. Leung, Stabilization of chaotic systems using linear sampled-data controller, *Int. J. Bifurcat. Chaos*, **17** (2007), 2021–2031. https://dx.doi.org/10.1142/S0218127407018191

35. X. L. Zhu, B. Chen, D. Yue, Y. Wang, An improved input delay approach to stabilization of fuzzy systems under variable sampling, *IEEE T. Fuzzy Syst.*, **20** (2012), 330–341. https://dx.doi.org/10.1109/TFUZZ.2011.2174242

36. Z. G. Wu, P. Shi, H. Su, J. Chu, Sampled-data fuzzy control of chaotic systems based on T-S fuzzy model, *IEEE T. Fuzzy Syst.*, **22** (2014), 153–163. https://dx.doi.org/10.1109/TFUZZ.2013.2249520

37. Z. P. Wang, H. N. Wu, On fuzzy sampled-data control of chaotic systems via a time-dependent Lyapunov functional approach, *IEEE T. Cybernetics*, **45** (2015), 819–829. https://dx.doi.org/10.1109/TCYB.2014.2336976

38. T. H. Lee, J. H. Park, New methods of fuzzy sampled-data control for stabilization of chaotic systems, *IEEE T. Syst. Man Cy. Syst.*, **48** (2018), 2026–2034. https://dx.doi.org/10.1109/TSMC.2017.2690803

39. Q. Inc, *Inverted pendulum experiment-SRV02 RTOPEN user manual*, Ontario, Canada, 2012. Available from: `https://www.quanser.com/products/rotary-inverted-pendulum/`.

40. K. J. Åström, K. Furuta, Swinging up a pendulum by energy control, *Automatica*, **36** (2000), 287–295. http://dx.doi.org/10.1016/S0005-1098(99)00140-5

AIMS Press